Drag reduction by microbubble injection in a channel flow

C. del C. Gutiérrez Torres
Instituto Politécnico Nacional, SEPI-ESIME Zacatenco,
U.P. Adolfo López Mateos Edif. 5, 3er Piso Col. Lindavista, 07738,
e-mail: cgutierrezt@ipn.mx

Y.A. Hassan
Texas A&M University, Collage Station, Tx. 77843-3133,
e-mail: y-hassan@tamu.edu

J.A. Jiménez Bernal
Instituto Politécnico Nacional, SEPI-ESIME Zacatenco,
U.P. Adolfo López Mateos Edif. 5, 3er Piso Col. Lindavista, 07738,
e-mail: jjimenezb@ipn.mx

J.G. Barbosa Saldaña
Instituto Politécnico Nacional, SEPI-ESIME Zacatenco,
U.P. Adolfo López Mateos Edif. 5, 3er Piso Col. Lindavista, 07738,
e-mail: jbarbosas@ipn.mx

Recibido el 26 de marzo de 2007; aceptado el 24 de enero de 2008

The injection of microbubbles within the turbulent boundary layer in a channel is investigated to elucidate the drag reduction phenomenon. Experimental data for a fully developed flow were obtained using the Particle Image Velocimetry (PIV) technique for single-and two-phase flow. Both cases are compared to examine the effects of the presence of microbubbles within the boundary layer, specifically the modification of vorticity, vortex structures, and fluctuating rate of strain, which is directly related to the energy dissipation in turbulent flows. A notorious decrease in the rate of strain as well as vorticity was observed for the two-phase flow. These results are significant and will help to reveal the physical mechanism of drag reduction by injection of microbubbles.

Keywords: Microbubbles; drag reduction; channel flow.

La inyección de microburbujas en la capa límite turbulenta en el flujo dentro de un canal es investigada para entender el fenómeno de reducción del arrastre. Resultados experimentales en un flujo totalmente desarrollado dentro de un canal cerrado fueron obtenidos utilizando la técnica de Velocimetría por Imágenes de Partículas (PIV) para una sola fase y dos fases. Ambos casos son comparados para analizar los efectos de la presencia de las microburbujas dentro de la capa límite. Específicamente las modificaciones en la vorticidad, vórtices y tasa de deformación. Esta última directamente relacionada con la disipación de energía en flujo turbulento. Estos resultados son significativos y pueden ayudar a entender de manera más precisa el mecanismo físico de la reducción del arrastre por inyección de microburbujas.

Descriptores: Microburbujas; reducción del arrastre; flujo en un canal.

PACS: 47.60.+i

1. Introduction

Continuous research of methods to reduce the drag in turbulent flows has been carried out for the past few decades. The injection of microbubbles is one of the most researched methods for achieving drag reduction. However, a consensus on the mechanism that governs this phenomenon has not been reached in spite of the efforts of several research groups.

Since the pioneering work of McCormick and Bhattacharyya [1], several parameters on the drag reduction by microbubble injection have been taken into account and several hypotheses about the governing mechanism have been formulated.

The speed of fluid has been considered as a parameter of influence on this phenomenon, whereas Merkle and Deutsh [2] suggested that fluid speeds where convective times are short compared to buoyant or turbulent diffusion increased the reduction of drag, McCormick and Battacharyya [1], and Kodama, *et al.* [3] agreed that the drag reduction effect decreases as the fluid speed increases.

The effect of the bubble size has been completely discarded as an important parameter in the drag reduction phenomenon by Moriguchi and Kato [4]. However, this is in complete disagreement with results reported by Xu *et al.* [5], who discovered that smaller bubbles produced a sustained drag reduction effect while larger bubbles only produced a transitory drag reduction effect. Merkle and Deutsh [2] found that the ideal bubble size to achieve drag reduction is not fixed, but related to the flow characteristics, $i.e.$ bubbles have to have a size between an order of magnitude larger than the thickness of the viscous sublayer, and an order of magnitude smaller than the thickness of the boundary layer.

Microbubbles were found to be more effective in obtaining a reduction in drag when they were located in the buffer

layer (Madavan *et al.* [6], Merkle and Deutsh [2], Kanai and Miyata [7], Guin *et al.* [8], Jiménez-Bernal *et al.*, [9], Dominguez-Ontiveros *et al.* [10], Zhen and Hassan [11], Hassan, et al. [12]), which is different from the suggestion presented by McCormick and Bhattacharyya, who stated that the presence of microbubbles in the viscous sublayer is the origin of the drag reduction.

The influence of the void fraction in the drag reduction phenomenon has been discussed by several researchers. Merkle and Deutsh [2], Kodama *et al.* [3], Moriguchi and Kato [4], Jiménez-Bernal et al., [9], Dominguez-Ontiveros *et al.* [10], Zhen and Hassan [11], Hassan, *et al.* [12] all agree that the drag reduction increases as the void fraction increases. However, Kanai and Miyata [7] stated that this effect is only present if the void fraction increases near the wall. Furthermore, Madavan *et al.* [6] found that increasing the void fraction increases the drag reduction but only to a certain point, since it was found that the effect of additional bubbles decreases as the fraction of bubbles in the boundary layer increases.

Several possible explanations for drag reduction produced by microbubbles have been stated. McCormick and Bhattacharyya [1] suggested that a disruption in the viscous sublayer by the microbubbles eliminates the high shear region close to the wall. Also, as the bubbles were convected away from the surface to the outer regions of the boundary layer, it was implied that they reduced the Reynolds stresses by absorbing the momentum by their elasticity.

Madavan *et al.* [6] attributed the drag reduction effect to a viscosity and density change, whereas Merkle and Deutsh [2] explained the drag reduction effect as a destruction of energy producing fluctuations near the buffer region by the microbubbles. This would result in the growth of the sublayer thickness as a manifestation of the drag reduction.

Guin *et al.* [8] stated that the drag reduction phenomenon was essentially inner region dependent. Kanai and Miyata [7] also observed a reduction of turbulent energy and streamwise velocity fluctuation in agreement with observations of Kitagawa *et al.* [13]; those results were attributed to the prevention of formation of the sheet-like structure of the spanwise vorticity.

Xu *et al.* [5] attributed the drag reduction effect to three causes, namely: density effects (in agreement with Madavan *et al.*), a reduction in turbulent momentum transfer (in agreement with McCormick and Bhattacharyya) and phenomena related to the direct interaction of microbubbles and turbulence.

A modification in the energy distribution due to the presence of microbubbles was observed by Jiménez-Bernal *et al.*, [9], Zhen and Hassan [14], and Hassan *et al.* [12]. A shift of energy distribution was also observed from high wave-numbers (smaller scales) to low wave-numbers (larger scales), as well as an increase in the integral time scale for the streamwise velocity when microbubbles are present.

Although several research studies have been conducted on the microbubble drag reduction phenomenon, there is still a lack of understanding about the physical mechanism involved in the reduction of drag due to the presence of microbubbles within the boundary layer. Since the reduction of drag is not the only effect observed in the presence of microbubbles, the analysis of some other effects produced by the presence of microbubbles can be a vehicle to achieve a better understanding of this phenomenon.

In this work, changes in the fluctuating strain rate, swirling strength and vorticity due to the presence of microbubbles are discussed. The relationship between the strain rate and the turbulent dissipation makes these results important, because they show that microbubbles have more than a single effect on the boundary layer dynamics for turbulent flows.

2. Experimental set-up

The experiments were performed in a rectangular acrylic channel (L = 4.8 m, W = 20.5 cm , h = 2.8 cm). Water was used as the working fluid and driven through the channel by gravity.

Two-dimensional velocity full fields were obtained for single-phase and two-phase flows (water and microbubbles) with a Reynolds number of 5128 (based on the bulk velocity and half height of the channel) by particle image velocimetry (PIV) technique. Images were recorded for a time span of approximately 3.3sec. Two hundred images (i.e. one hundred velocity fields) were recorded for each set.

Hydrogen microbubbles were produced by electrolysis and injected into the turbulent boundary layer. A detailed description of the experimental set-up as well as detailed diagrams of it can be found in Refs. 9, 10, 11, 12, and 14.

3. Experimental results and discussion

To elucidate the effects of the microbubbles' presence within the boundary layer, several parameters were evaluated and their changes were monitored after the injection of microbubbles.

3.1. Boundary layer thickness

One of the first changes in the turbulent flow structure in a channel flow when microbubbles are injected is the change in boundary layer thickness. To evaluate these changes, the thickness of the boundary layer for single-phase and two-phase flow with a void fraction of 4.4% and 4.9% were evaluated. The boundary layer thickness (δ_{99}) was obtained considering the distance from the wall where the mean velocity is within 1% of the free stream velocity [15].

Changes were observed in the thickness of the viscous sublayer ($y^+ < 5$), and the buffer layer ($5 < y^+ < 30$), both defined in wall units.

TABLE I. Thickness of the boundary layer under different void fraction conditions.

Void fraction [%]	δ_{99}[mm]	Viscous sublayer thickness (y^+ <5) [mm]	Buffer layer thickness (5<y^+<30) [mm]
0 (single phase)	3.63	0.43	2.57
4.4%	3.96	0.52	3.09
4.9%	4.04	0.55	3.29

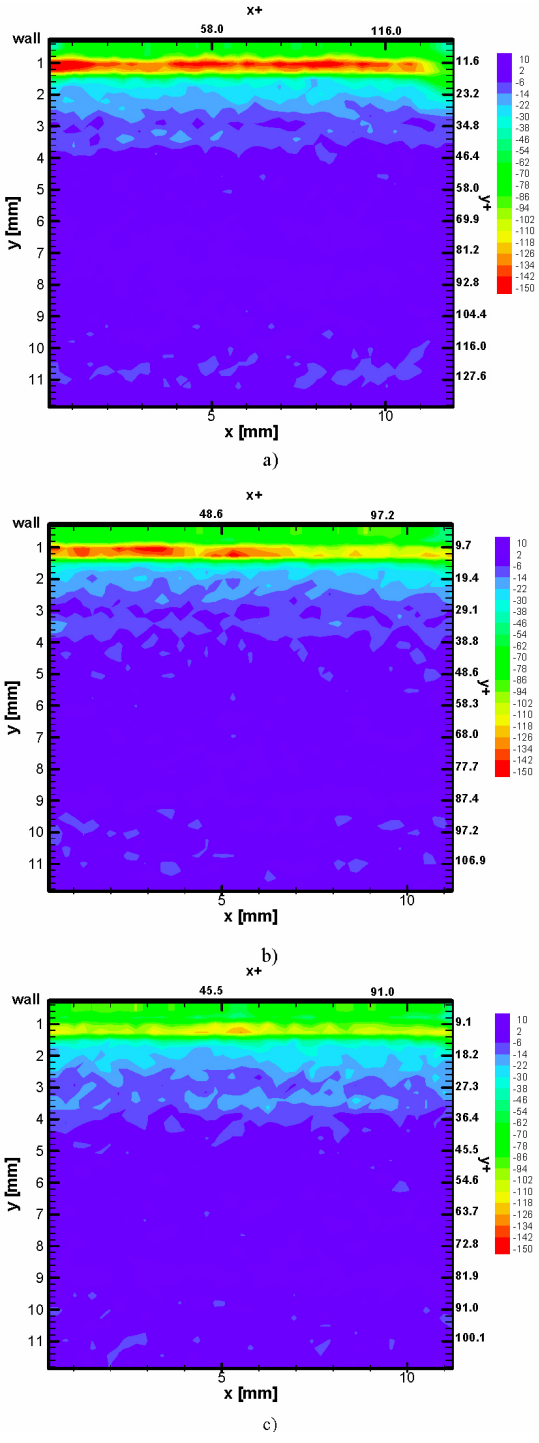

FIGURE 1. Z-component of average vorticity for a) single-phase flow, b) two-phase flow α=4.4%, DR=29.8% and b) two phase flow α=4.9%, DR=38.4%.

In this case y^+ is defined as $y^+ = u_\tau y/\nu$, where u_τ is the friction velocity $u_\tau = (\tau_w/\rho)^{1/2}$, and ν is the kinematic viscosity.

The void fraction within the viewing area is defined as

$$\alpha = \frac{V_g}{V_l + V_g} x100,$$

V_g = volume of gas within the viewing area and V_l = volume of liquid.

The effect of the presence of microbubbles within the boundary layer is a decrease in drag. The drag reduction, DR, is calculated by

$$DR = 1 - \frac{\tau_{w,water \text{ and bubbles}}}{\tau_{w,water}},$$

where the wall shear stress τ_w is measured from PIV using,

$$\tau_w = \mu \frac{dU}{dy}\bigg|_{y=0}.$$

As the void fraction increases, there is an increase in the boundary layer thickness. Likewise, an increase in both the viscous sublayer and the buffer layer thickness is observed. These changes are presented in Table I.

These results are similar to the data reported by Mercke and Deutsh [2]. A growth in the sublayer thickness were observed as well as a drag reduction effect.

3.2. Vorticity evaluation

The presence of vorticity is essential to the dynamics of turbulence. Non-linearity, rotationality ($\omega \neq 0$) and dimensionality (the three-dimensional character of turbulence) interact dynamically to feed the turbulence [16].

Wall shear stress and vorticity are directly related. When the wall shear stress is high, the vorticity is large. Therefore, a decrease in the wall shear stress should be accompanied by a decrease in vorticity.

In this experiment, the streamwise (u) and the normal (v) velocity components are measured. Therefore, the z-component of the vorticity was calculated. The z-vorticity (spanwise) component in the near wall region is calculated using:

$$\overrightarrow{\omega}_z = \left(\frac{\partial u}{\partial y} - \frac{\partial v}{\partial x}\right) \quad (1)$$

To calculate velocity derivatives, a central difference scheme was applied to PIV results. Experimental results for

the average z-component of vorticity, obtained for 100 velocity fields, for the single-phase case and the two-phase flow with a void fraction of 4.4% and 4.9% are shown in Fig. 1.

Likewise, the fluctuating vorticity was also calculated, and instantaneous results for z-fluctuating vorticity are shown in Fig. 2.

In Figs. 2b and 2c, the location of microbubbles is also shown. However, they are not show to scale. It can be observed that the presence of microbubbles reduced the intensity of the vorticity field, altering the original flow field.

In both cases (average and fluctuating vorticity) the same effect is observed, a decrease in vorticity as the void fraction increases. It is clearer for the average vorticiy results that for the single-phase flow there seems to be a sheet-like structure close to the wall. As the void fraction grows, this effect is weakened by the presence of microbubbles. This observation is in agreement with Kitagawa *et al.* [13] that attributed the drag reduction effect to the prevention of the formation of a sheet-like structure of the spanwise vorticity.

3.3. Vortex Identification

Detection and characterization of vortical elements and structures constitutes a significant portion of the studies carried out to get a better understanding of the boundary layer structure in turbulent flows. Its importance lies in the fact that a vortex with an orientation different from a wall-normal one has the potential to transport mass and momentum across the mean velocity gradient [17].

Identification of vortices in a velocity field is normally carried out using vorticity. However, vorticity not only identifies vortex cores, but also regions of significant shear that frequently mask the presence of vortices. Furthermore, vorticity is a point function, whereas the properties of a fluid in a state of vortex motion cannot be described with reference to a single point in space; they cannot be expressed by a differential operator [18].

The use of swirling strength in two-dimensional PIV fields for vortex identification was reported by Adrian *et al.* [19]. In that work, this method was applied to instantaneous PIV velocity fields with and without the presence of microbubbles within the boundary layer in a channel flow to elucidate the effects of the presence of microbubbles in the vortical structure in a near-wall region.

The swirling strength technique to localize vortex in a flow field is based on the premise that in three dimensions, the local velocity gradient tensor will have a real eigenvalue (λ_r) and a pair of complex conjugate eigenvalues $(\lambda_{cr} \pm i\lambda_{ci})$ when the discriminant of its characteristic equation is positive. When$\lambda_{ci} > 0$, it corresponds to quasi-circular ellipses followed by the particles as trajectories of their movements. The strength of any local swirling motion is quantified by(λ_{ci}), defined as the swirling strength of the vortex.

For two-dimensional PIV velocity fields, the full tensor cannot be formed. Adrian *et al.* proposed the use of an equivalent two-dimensional form of this tensor; namely,

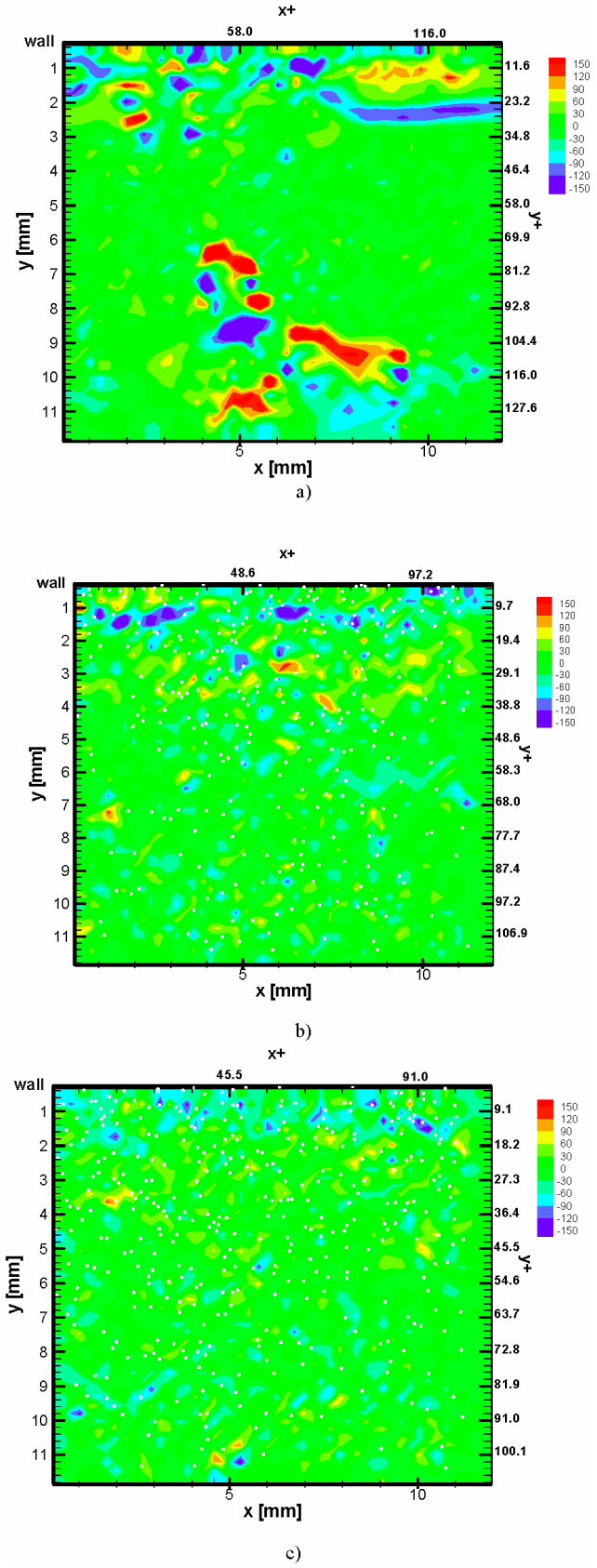

FIGURE 2. Z-component of instantaneous fluctuating vorticity for a) single-phase flow, b) two-phase flow α=4.4%, DR=29.8% and b) two-phase flow α=4.9%, DR=38.4%.

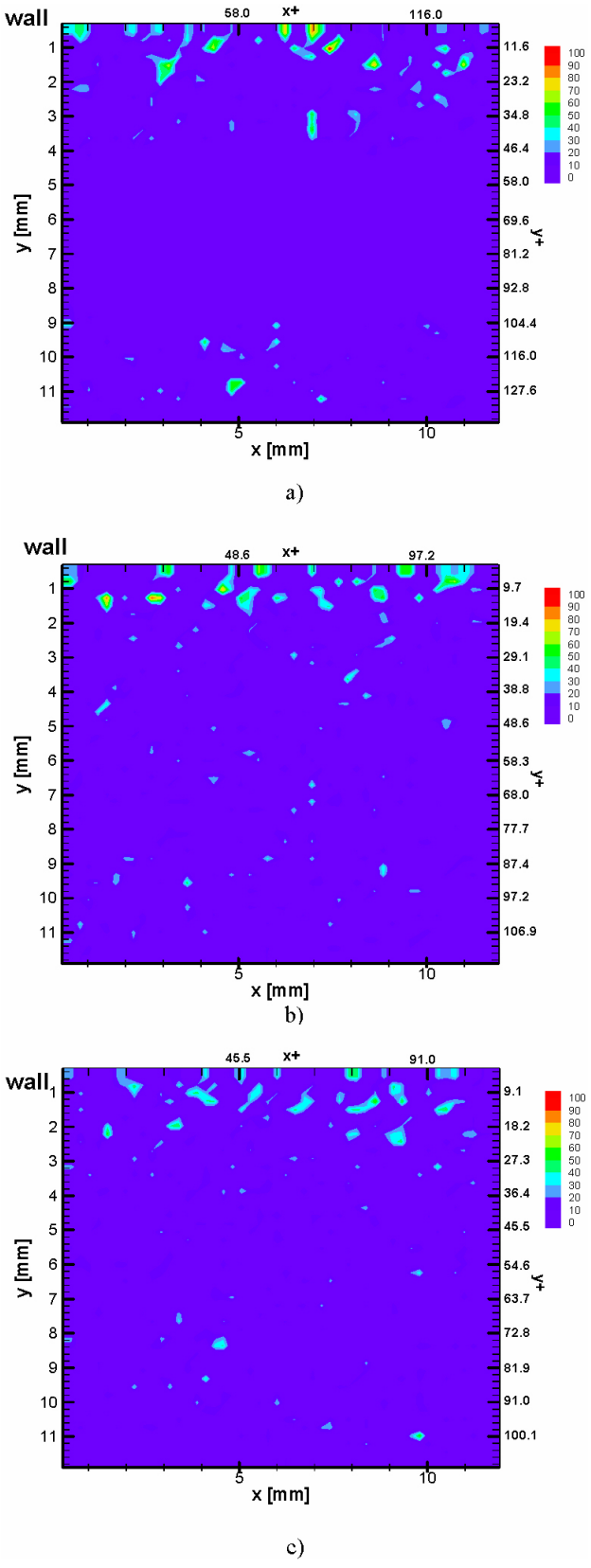

FIGURE 3. Swirling strength instantaneous maps a) single-phase flow, b) two-phase flow α=4.4%, DR=29.8% and b) two-phase flow α=4.9%, DR=38.4%.

$$\underline{\underline{D}}^{2-D} = \begin{bmatrix} \frac{\partial u}{\partial x} & \frac{\partial u}{\partial y} \\ \frac{\partial v}{\partial x} & \frac{\partial v}{\partial y} \end{bmatrix} \tag{2}$$

where u and v correspond to the instantaneous velocity components in the streamwise and normal directions, respectively. In this case, $\underline{\underline{D}}^{2-D}$will have either two real eigenvalues or a pair of complex conjugate eigenvalues. Vortices can be identified by plotting regions with constant values of $\lambda_{ci} > 0$. Figure 3 shows a comparison for the swirling strength results in a single-phase flow and the values of the local void fraction of 4.4 and 4.9%, which correspond to DR = 29.8% and DR = 38.4% respectively.

Changes in size, distribution and intensity for the vortex found in single-and two-phase flow can be attributed to the presence of microbubbles, and could explain the reduction in drag due to a decrease in mass and momentum transport across the mean velocity gradient. However, due to the limitations of the experiment (measurements were taken in the x-y plane close to the wall only), it is not possible to state that the vortex orientation is different from a wall-normal one. The changes observed could also be explained as a change in vortex orientation due to presence of microbubbles, so further experimentation is needed to completely explain this behavior modification.

3.4. Fluctuating strain rate

In turbulent flows, the dissipation of energy $\varepsilon = 2\nu\overline{s_{ij}s_{ij}}$, is associated with the symmetric part of the velocity derivative tensor $\partial u_i/\partial x_j$ [20]. The fluctuating strain rate is defined by

$$s_{ij} = \frac{1}{2}\left(\frac{\partial u_i}{\partial x_j} + \frac{\partial u_j}{\partial x_i}\right). \tag{3}$$

Energy dissipation is due to viscous stresses and the local strain rate, and takes place at the smallest scales in turbulent flows. However, the amount of dissipation is governed by the large, energy-containing eddies because the rate energy is taken from the mean flow to enter the turbulence, and the rate energy leaves the large scales for the next smaller scales, is always determined by the large scale dynamics. When this energy finally reaches the smallest dissipative scales, the rate of dissipation can no longer be influenced [16].

Figure 3 shows results for a single phase and local void fraction of 4.4 and 4.9%, which corresponds to DR = 29.8% and DR = 38.4.4%, respectively, for a fluctuating rate of strain field. The fluctuating strain rate is multiplied by itself and averaged in time($\overline{s_{ij}s_{ij}}$). In this case, just the s_{12} component, $i.e.$ the z-component, can be obtained since the PIV measurements are carried out only in the x-y plane. The gradient evaluations in Eq. (3) were computed using the central difference scheme.

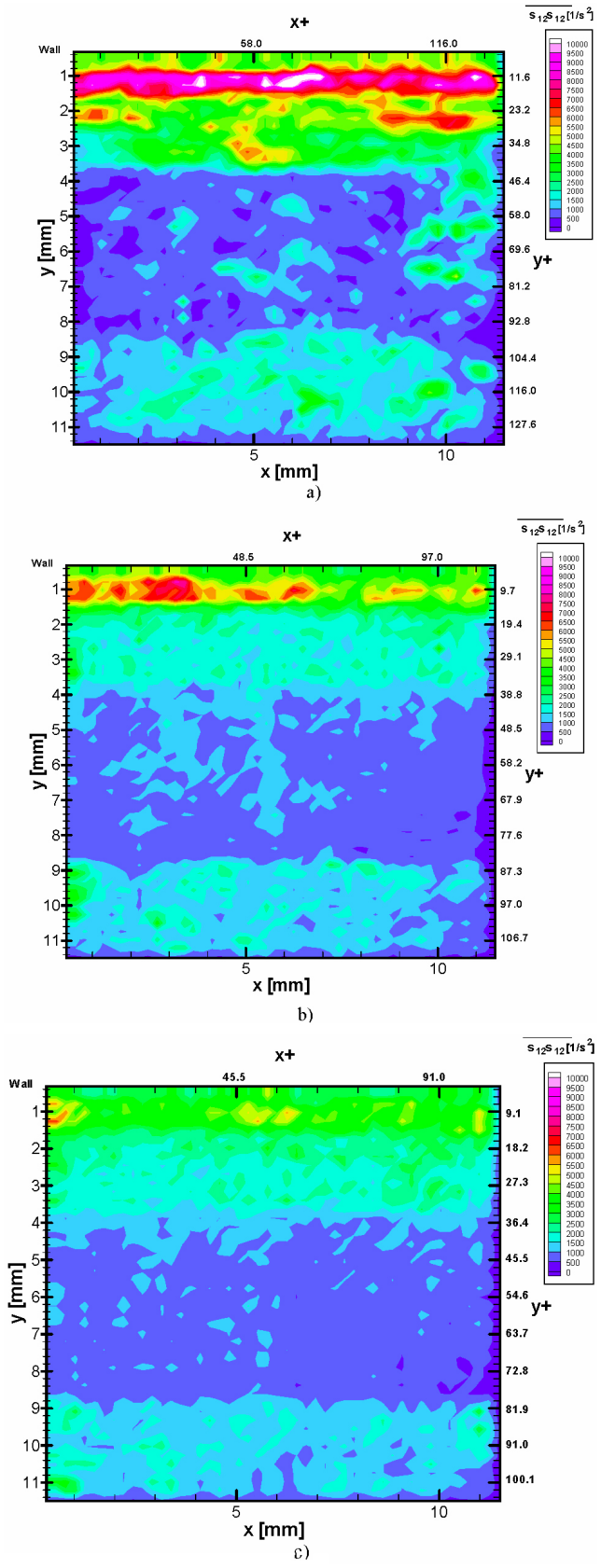

FIGURE 4. $\overline{s_{12}s_{12}}$ distribution for a) single phase flow, b) two phase flow α=4.4%, DR=29.8% and b) two phase flow α=4.9%, DR=38.4%.

A significant change can be observed from Fig. 4a. to 4b. This change in the fluctuating strain rate is very important because it can translated into an energy dissipation decrease, which is a very meaningful consequence of the presence of microbubbles within the boundary layer.

4. Conclusions

The presence of microbubbles within the boundary layer produces a growth in the boundary layer, viscous sublayer, and buffer layer thickness, which is in agreement with findings of other researchers [2,6]. A decrease is also observed in the z-vorticity component. This is a consequence of a decrease in the wall shear stress. The decrease of the vorticity in the near-wall region also indicates a decrease in strain, which leads to a suppression of the Reynolds stresses. All of these changes lead to a decrease in drag. A modification in the vortical structures close to the wall can be observed by the evaluation of both fluctuating spanwise vorticity and swirling strength. These changes could be explained as a decrease in the momentum exchange across the main velocity gradient due to the presence of microbubbles. However, from the results obtained, it cannot be stated beyond a doubt because the orientation of the vortices is not completely determined. If a decrease in momentum exchange were the explanation, the role of the presence of microbubbles acting as a barrier for the continuous phase momentum exchange would help to explain the drag reduction phenomenon. The changes in the fluctuating spanwise vorticity fields also suggest a decrease of zones in strong shear within the boundary layer.

Another important finding is the decrease in the fluctuating strain rate in the presence of microbubbles. This can be easily translated into a reduction in the turbulent energy dissipation. The decrease in energy dissipation due to the presence of microbubbles cannot be directly explained by a change in viscosity or density, first because changes in viscosity only produce a change in dissipation scale [16], secondly because the dissipation of energy is determined by the rate of energy withdrawal from the main flow, and finally because viscosity and density are scalar properties of the fluid that can alter the dissipation scale (through changes in the kinematic viscosity) but that cannot change the rate of strain that depends on velocity gradients throughout the flow field. Furthermore, previous results showing a change in the dynamics of the energy cascade due to the presence of microbubbles, were reported in Ref. 9, where a shift in energy contain was found from higher wavenumber to lower wavenumber scales (change in length scales for eddies). The same shift was reported in Ref. 14 using a wavelet analysis technique, and changes (increase) in the time scale were found in the presence of microbubbles[12]. Therefore, it can be concluded that the presence of microbubbles modifies the dynamics in the boundary layer, changing the scale of the energy-containing eddies to a larger one, increasing the time scale of those eddies and decreasing the rate of strain and consequently the dissipation rate.

1. M.E. Mccormick and R. Bhattacharyya, *Naval Engineers Journal* **April** (1973) 11.
2. C.L. Merkle and S. Deutsch, *Frontiers in Experimental Fluid Mechanics Sen. Lecture Notes in Engineering* **46** (1989) 291.
3. Y. Kodama, A. Kakugawa, T. Takahashi, and H. Kawashima, *Int. J. Heat and Fluid Flow* **21** (2000) 582.
4. Y. Moriguchi and H. Kato, *Journal of Marine Science and Technology* **7** (2002) 79.
5. J. Xu, M.R. Maxey, and G.E. Karniadakis, *J. Fluid Mech*. **468** (2002) 271.
6. Madavan, N. K., Merkle, C.L. and Deutsch, S., *J. Fluids Eng. Transactions of ASME* **107** (1985) 370.
7. A. Kanai & H. Miyata, *Int. J. Numer. Meth Fluids* **35** (2001) 593.
8. M.M. Guin, H. Kato, H. Yamaguchi, M. Maeda, and M. Miyanaga, *Journal of Marine Science and Technology* **1** (1996) 241.
9. J.A. Jiménez-Bernal, Y.A. Hassan, and C.C. Gutiérrez-Torres, *Transactions of the American Nuclear Society* **91** (2004) 237.
10. E.E. Domínguez-Ontiveros, C.E. Estrada-Pérez, J.A. Jiménez-Bernal, and Y.A. Hassan, *Transactions of the American Nuclear Society* **91** (2004) 232.
11. L. Zhen, and Y.A. Hassan, *Transactions of the American Nuclear Society* **91** (2004) 230.
12. Y.A. Hassan, C.C. Gutiérrez-Torres, J. Jiménez-Bernal, *Internacional Communications in Heat and Mass Transfer* **32** (2005) 1009.
13. A. Kitagawa, K. Hishida, and Y. Kodama, *Experiments in Fluids* **38** (2005) 466.
14. L. Zhen and Y.A. Hassan, *Chemical Engineering Science* **61** (2006) 7107.
15. P.S. Bernard and J.M. Wallace, *Turbulent Flow Analysis, Measurement and Prediction*, 1^{st}. Edition (John Wiley and Sons, United States of America, 2002).
16. P. Holmes, J.L. Lumley, and G. Berkooz, *Turbulence, Coherent Structures, Dynamical Systems and Symmetry*, 1^{st}. Edition (Cambridge University Press, United Kingdom, 1996).
17. S.K. Robinson, *Annu. Rev. Fluid Mech.* **23** (1991) 601.
18. H.J. Lugth, *The dilemma of defining a vortex, In:Recent developments in theoretical and experimental fluid mechanics* ed. V. Muller, K.G. Roesner, and B. Schmidt (Berlin: Springer-Verlag, 1979) p. 309.
19. R.J. Adrian, K.T. Christensen, and Z. –C. Liu, *Experiments in fluid* **29** (2000) 275.
20. A. Tsinober, *An Informal Introduction to Turbulence*, 1^{st}. edition (Kluwer Academic Publishers, Dordrecht, The Netherlands, 2001).